




Relation between structure conversion and spectratuning properties of Eu^{2+} -doped strontium aluminate phosphor

Biao Zhang¹, Quansheng Liu^{1,*} , Wenjie Yan¹, Yulong Chen¹, Anfeng Shen¹, and Haihan Zhang¹

¹ School of Materials Science and Engineering, Changchun University of Science and Technology, Changchun 130012, Jilin, China

Received: 21 November 2016

Accepted: 20 March 2017

Published online:
28 March 2017

© Springer Science+Business
Media New York 2017

ABSTRACT

Phosphors based on strontium aluminates activated by Eu^{2+} ions with various Al/Sr ratios were synthesized by a traditional high-temperature solid-state method. The influences of Al/Sr ratio, sintering temperature, the doping concentration of europium ions on structural transformation and luminescent properties of the phosphors were studied. The quenching and luminescent mechanisms were also discussed. The optimum synthetic temperature and time are about 1350 °C and 3.5 h derived from the analysis and experiment. At the range of Al/Sr ratio from 1.5 to 4.0, there are only three crystal structures, $\text{Sr}_3\text{Al}_2\text{O}_6$ (1.5) cubic structure, SrAl_2O_4 (2.0–3.0) monoclinic crystal system and $\text{Sr}_4\text{Al}_{14}\text{O}_{25}$ (3.0–4.0) orthorhombic crystal system. Under UV light excitation, the emission peaks gradually generate blueshift from 510 nm of $\text{Sr}_3\text{Al}_2\text{O}_6:\text{Eu}^{2+}$ phosphor to 483 nm of $\text{Sr}_4\text{Al}_{14}\text{O}_{25}:\text{Eu}^{2+}$ phosphor and the two emission peaks are originated from $4f^65d^1$ to $4f^7$ intrinsic transition of Eu^{2+} ions. The best green and blue luminescent samples are $\text{SrAl}_2\text{O}_4:\text{Eu}^{2+}$ and $\text{Sr}_4\text{Al}_{14}\text{O}_{25}:\text{Eu}^{2+}$, and their color purity is 0.6667 and 0.8229, respectively. The best doping amount of Eu^{2+} is 0.5 at.%, and the concentration quenching mechanism of Eu^{2+} ions in $\text{SrAl}_2\text{O}_4:\text{Eu}^{2+}$ and $\text{Sr}_4\text{Al}_{14}\text{O}_{25}:\text{Eu}^{2+}$ phosphors can be ascribed to the dipole–dipole interaction. There are three types of 6, 7 and 10 coordination numbers around $\text{Sr}^{2+}(\text{Eu}^{2+})$ ion, which forms three types of polyhedras, resulting in generating three excitation peaks at 334, 368 and 430 nm corresponding to the 6, 7 and 10 coordination polyhedral. The relation between energy level splitting and coordination number can be expressed as E_6 (6-coordination) $>$ E_7 (7-coordination) $>$ E_{10} (10-coordination) in aluminate phosphor, and the splitting width of 6, 7 and 10 coordination numbers is 1.29, 0.78 and 0.31 eV, respectively. The coordination field only affects the energy top of crystal field splitting, and the larger the coordination number is, the lower the energy level top of crystal field splitting in $\text{Sr}_4\text{Al}_{14}\text{O}_{25}:\text{Eu}^{2+}$ phosphor is.

Address correspondence to E-mail: liuqs@cust.edu.cn

Introduction

Luminescent materials have been extensively investigated in recent years because of their manifold range of potential application, such as color display technologies, high-efficiency solid-state lighting, information storage, biological sensing, and labeling, photoelectronic and photonic devices [1]. Rare-earth-ions-doped phosphors as a stable and high-efficient luminescent materials have become the mainstream orientation in luminescent material. The Eu^{2+} ions-doped strontium aluminate luminescent materials, in particular, have attracted increasing attention due to its superior luminescent properties, abundant sorts, lower cost, stable chemical performance, etc. [2]. Palilla et al. [3] firstly found $\text{SrAl}_2\text{O}_4:\text{Eu}^{2+}$ green luminescent materials. Strontium aluminate (SrAl_2O_4) phosphors have been paid more attention because they have the high quantum efficiency, considerable thermal and chemical stability [4]. Matsuzawa et al. [5] improved the luminescent intensity of phosphor by Eu^{2+} and Dy^{2+} codoping. Then, all kinds of alkaline earth metal aluminate systems based on $\text{MAl}_2\text{O}_4:\text{Eu}^{2+}$ ($\text{M} = \text{Ca}, \text{Sr}, \text{Ba}$) have aroused wide concern [6, 7]. Sahu et al. [8] pointed the crystal structures of the prepared phosphors were consistent with standard monoclinic phase with a space group $\text{P}2_1$ and the $\text{SrAl}_2\text{O}_4:\text{Eu}^{2+}$ phosphor would emit green light, belonging to the broad emission band ascribed to the $4f^65d^1-4f^7$ transition. Subsequently, various matrix strontium aluminate phosphors, such as $\text{Sr}_3\text{Al}_2\text{O}_6$ [9–11] and $\text{Sr}_4\text{Al}_{14}\text{O}_{25}$ [12–14], began to appear and they also have been investigated extensively. Chang et al. [15] studied the photoluminescence of Eu^{2+} , Dy^{3+} and Eu^{3+} , Dy^{3+} -codoped $\text{Sr}_3\text{Al}_2\text{O}_6$ phosphor and pointed out the emission peaks of Eu^{2+} , Dy^{3+} -codoped $\text{Sr}_3\text{Al}_2\text{O}_6$ phosphor is at 512 nm. Inan Akmeahmet et al. [16] studied the Eu^{2+} and Dy^{3+} -codoped $\text{Sr}_4\text{Al}_{14}\text{O}_{25}$ phosphors, discussed the influence of B-doping on structure, found the microstructural evolution, promoted more uniform distribution of the optically active of Eu^{2+} ion in the Sr^{2+} cation sublattice, and improved the phosphors luminescent intensity. Although all kinds of strontium aluminate matrix phosphors have been investigated, the relation between structural transition and spectral properties is scarcely reported in same synthetic conditions. In view of this, the $\text{Sr}_3\text{Al}_2\text{O}_6:\text{Eu}^{2+}$, $\text{SrAl}_2\text{O}_4:x\text{Eu}^{2+}$ and

$\text{Sr}_4\text{Al}_{14}\text{O}_{25}:x\text{Eu}^{2+}$ phosphors were synthesized by the traditional high-temperature solid-state reaction method via tuning Al/Sr ratio. The relation between structural transition and spectral property was established. The influence of Eu^{2+} ions content on the luminescent properties and quenching mechanism was also discussed.

Experimental

The phosphors with different Al/Sr ratios were synthesized via the traditional high-temperature solid-state reaction method. The starting materials are SrCO_3 (A.R.), Al_2O_3 (A.R.), H_3BO_3 (A.R.), Eu_2O_3 (99.99%) whose manufacturer is Sinopharm Chemical Reagent Co., Ltd (Shanghai). Firstly, the Al/Sr ratios of 1.5, 2.0, 2.5, 3.0, 3.5, 4.0 were designed. Then, according to the ratios, weigh some quantity of Al_2O_3 and SrCO_3 , add 1.0 at.% H_3BO_3 of the product weight as fluxing agent and weigh 0.2, 0.5, 0.8, 1.0, 1.4, 2.0, 4.0, 6.0, 8.0 at.% Eu_2O_3 as activator. Thirdly, these raw materials were mixed and ground thoroughly in an agate mortar for half an hour. Lastly, the mixture was placed into an alumina crucible and sintered at 1100 °C for 45 min, which makes SrCO_3 decompose enough, and then sintered at 1350 °C for 3.5 h in the reducing atmosphere. When finally cooling to room temperature, the phosphors were obtained.

The thermogravimetric (TG)/different scanning calorimeter (DSC) was monitored to determine the synthetic temperature by Netzsch STA449C at a heating rate of 10 K/min. X-ray power diffractions (XRD) were measured by Japan Rigaku D/max-IVB diffractometer, CuK_α , 40.0 kV, 20.0 mA, $\lambda = 0.15406$ nm, in order to establish the crystallization and phase transformation behavior of these phosphors. The emission and excitation spectra were characterized by Japan SHIMADZU RF-5301 fluorescence spectrophotometer, Xenon lamp, 150 W. All the measurements except TG/DSC were performed at room temperature.

Results and discussion

Thermal analysis

Figure 1 presents TG/DSC curves of raw materials synthesized $\text{SrAl}_2\text{O}_4:\text{Eu}^{2+}$ phosphor. It is obvious in the TG curve that the weight loss mainly takes place

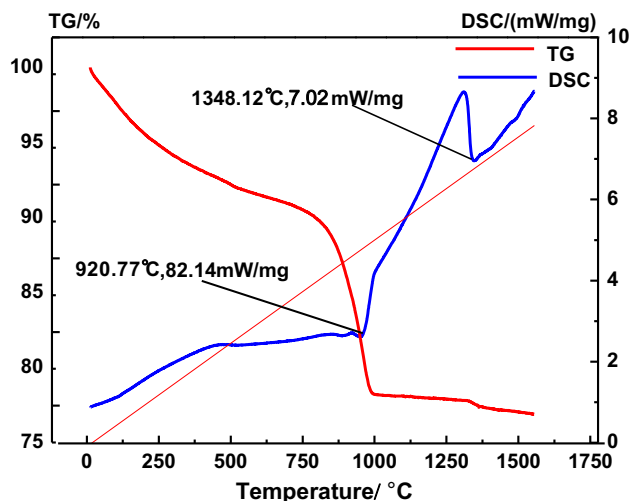


Figure 1 TG/DSC curves of raw materials for synthesis $\text{SrAl}_2\text{O}_4:\text{Eu}^{2+}$ phosphor.

in the range of room temperature to 1100 °C, and there is a significant weight loss occurred at 900–1000 °C for a decomposition process of SrCO_3 which produces carbon dioxide. There are one endothermic peak at 920.77 °C and one apparent exothermic peak at 1348.12 °C in the DSC curve, which are caused by the decomposition of SrCO_3 and the product crystallization of $\text{Sr}_x\text{Al}_y\text{O}_z:\text{Eu}^{2+}$ phosphor, respectively [17, 18]. In Fig. 1, it shows DSC and TG curves of the raw mixture. Obviously, from the DSC curve, there is an endothermic peak at 920.77 °C, which is identical with the temperature of the decomposition of SrCO_3 . Meanwhile, from the TG curve, there is a dramatic decline of weight at about 920 °C, because the decomposition of $\text{SrCO}_3(\text{SrCO}_3(\text{s}) \rightarrow \text{SrO}(\text{s}) + \text{CO}_2(\text{g}))$ releases the carbon dioxide and leads to the mass reduction. To sum up, the endothermic at 920.77 °C is caused by the decomposition of SrCO_3 . Combining TG/DSC curves and a great deal of experimental data, the calcination temperature of 1350 °C was adopted to ensure the prepared phosphor with various Al/Sr ratios. In order to determine the best calcination time, the various holding times were carried out for $\text{SrAl}_2\text{O}_4:\text{Eu}^{2+}$ phosphor and $\text{Sr}_4\text{Al}_{14}\text{O}_{25}:\text{Eu}^{2+}$ phosphor. The XRD patterns of $\text{SrAl}_2\text{O}_4:\text{Eu}^{2+}$ and $\text{Sr}_4\text{Al}_{14}\text{O}_{25}:\text{Eu}^{2+}$ phosphors calcined at 3, 3.5 and 4 h are displayed in Figs. S1 and S2 in supplemental file, respectively. The spectra of $\text{SrAl}_2\text{O}_4:\text{Eu}^{2+}$ and $\text{Sr}_4\text{Al}_{14}\text{O}_{25}:\text{Eu}^{2+}$ phosphors calcined at 3, 3.5 and 4 h are displayed in Figs. S3 and S4 in supplemental file, respectively. When the sintering

time is 3 h, the XRD patterns are chaotic and luminous intensity of phosphor is weak. When prolonging the sintering time, crystallized completeness of crystal structure is increasing, grains can grow up enough, and Eu^{2+} ions have enough time to enter the lattice to form more illuminant center. But, when it reaches 4 h, the phosphors over-burn and weaken the luminous intensity. Based on the data, the sintering time of 3.5 h was chosen for preparation phosphors.

The effects of Al/Sr ratio on structural and luminescent properties

Al/Sr ratio has significant effects on luminescent properties and phase component of $\text{Sr}_x\text{Al}_y\text{O}_z:\text{Eu}^{2+}$ phosphors. Figure 2 illustrates the XRD patterns of $\text{Sr}_x\text{Al}_y\text{O}_z:\text{Eu}^{2+}$ phosphors with different Al/Sr ratios (Al/Sr = 1.5, 2.0, 2.5, 3.0, 3.5 and 4.0). When Al/Sr ratio is 1.5, the diffraction peaks are accordant with that of $\text{Sr}_3\text{Al}_2\text{O}_6$ (PDF No. 24-1187), which indicates that the product is cubic structural $\text{Sr}_3\text{Al}_2\text{O}_6$ phase, and the cell parameter is 1.5844 nm with a Pa-3 space group. When Al/Sr ratio is 2.0, 2.5 and 3.0, by comparing with standard PDF card No. 34-0379, it is clear that the products belong to monoclinic crystal system of SrAl_2O_4 phase. And the sample of Al/Sr ratio is 2.0 and purer, indicating the crystallization is more complete. With further increase in Al/Sr ratio, the impure phase of $\text{Sr}_4\text{Al}_{14}\text{O}_{25}$ begins to appear. When Al/Sr ratio approaches 3.5 and 4.0, the main phase turns into $\text{Sr}_4\text{Al}_{14}\text{O}_{25}$ crystal structure, and the

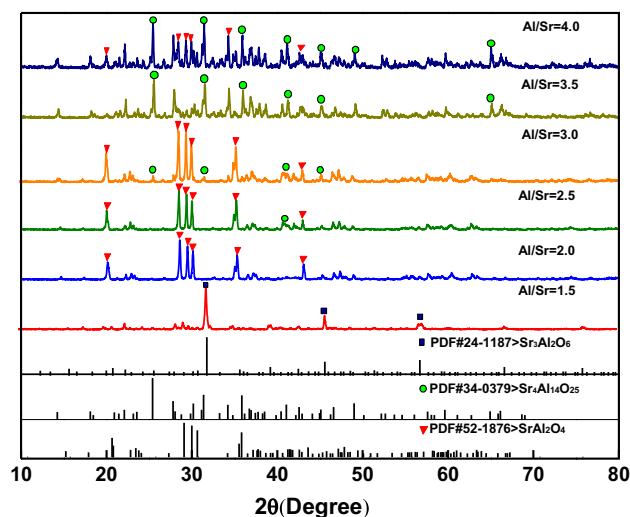


Figure 2 XRD patterns of $\text{Sr}_x\text{Al}_y\text{O}_z:\text{Eu}^{2+}$ phosphors with various Al/Sr ratio.

diffraction peaks are identical with the diffraction of PDF No. 52-1876, indicating that the crystal structure of products is orthorhombic crystal system with a Pmma space group, and the cell parameters are 2.4791, 0.8486 and 0.4886 nm. The pure phase of $\text{Sr}_4\text{Al}_{14}\text{O}_{25}$ can be obtained while the Al/Sr ratio is 3.5. There are no any diffraction peaks corresponding to Eu^{2+} ions for all samples, indicating the doping of Eu^{2+} ions has no effects on lattice of phosphors [19, 20]. It is true that the composition and structure of products are not completely same with original design (that is stoichiometric ratio). At the range of Al/Sr ratio from 1.5 to 4.0, there are only three structures, $\text{Sr}_3\text{Al}_2\text{O}_6$ (1.5) cubic structure, SrAl_2O_4 (2.0–3.0) monoclinic crystal system and $\text{Sr}_4\text{Al}_{14}\text{O}_{25}$ (3.0–4.0) orthorhombic crystal system. In view of the rule of crystal structure conversion, the orthorhombic structure could convert to monoclinic structure and also translate to cubic structure, so that the structure of $\text{Sr}_4\text{Al}_{14}\text{O}_{25}$ is unstable and difficult to get high-purity phase.

Figure 3 is the excitation (a) and emission (b) spectra of $\text{Sr}_x\text{Al}_y\text{O}_z:\text{Eu}^{2+}$ phosphors with Al/Sr ratio of 1.5, 2.0, 2.5, 3.0, 3.5 and 4.0. Excitation wavelength is 368 nm, and the monitored wavelength measured in excitation spectra is the wavelength of samples luminescent peak value. It is obvious that there are only two types of spectra properties in spite of three types of products. With Al/Sr increasing from 1.5 to 3.5, the luminous intensity of material increased gradually. When Al/Sr

Sr ratio equals to 3.5, the luminous intensity of the phosphor is the highest. However, when Al/Sr continuously increases from 3.5 to 4.0, the luminous intensity of the phosphor reversely decreases obviously. It is the fact that the optimum luminescent sample is $\text{Sr}_4\text{Al}_{14}\text{O}_{25}:\text{Eu}^{2+}$ phosphor. For the green light peaking at 510 nm, the $\text{SrAl}_2\text{O}_4:\text{Eu}^{2+}$ sample is superior to the $\text{Sr}_3\text{Al}_2\text{O}_6:\text{Eu}^{2+}$ sample, the luminescent intensity of $\text{Sr}_3\text{Al}_2\text{O}_6:\text{Eu}^{2+}$ phosphor is lowest, and the shape and the position of peak have no differences with $\text{SrAl}_2\text{O}_4:\text{Eu}^{2+}$ phosphor. In addition, the emission peak gradually shifts to the short wavelength (blueshift) from 510 to 483 nm with increasing Al/Sr ratio and the blueshift is 27 nm. In view of this, we will discuss the $\text{Sr}_4\text{Al}_{14}\text{O}_{25}:\text{Eu}^{2+}$ and the $\text{SrAl}_2\text{O}_4:\text{Eu}^{2+}$ phosphors by the following [21–23]. When Al/Sr ratio is <2.5 , the phosphors emit green light and the emission spectra of phosphors are broadband spectra peaking approximately at 510 nm caused by $4f^65d^1-4f^7$ transition, the excitation spectra are also a wideband spectra from 300 to 410 nm, only one excitation peak near at 345 nm caused by the transition of $4f^7$ ground state to $4f^65d^1$ excitation state of Eu^{2+} ions, and the width of the excitation band approaches 110 nm. While Al/Sr ratio is more than 3.0, the phosphors emit Cambridge blue light, and the emission spectra are also wide band from 430 to 540 nm peaking at 483 nm ascribed to $4f^65d^1-4f^7$ intrinsic transition of Eu^{2+} ions, but the excitation spectra have two excitation peaks near at 368 and 430 nm, respectively, and one excitation band

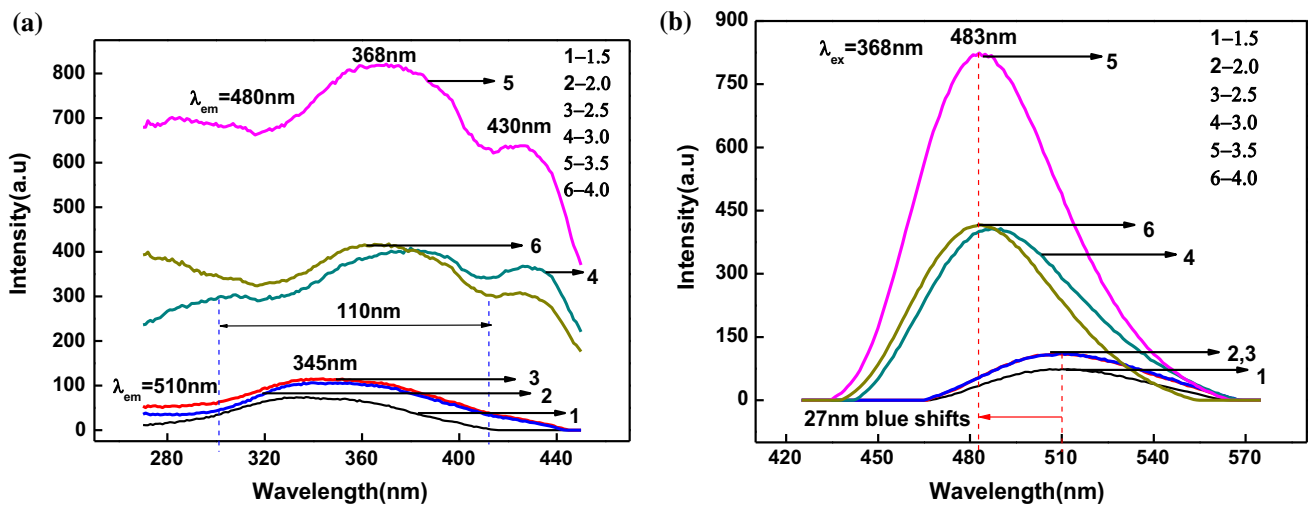


Figure 3 Excitation (a) and emission (b) spectra of $\text{Sr}_x\text{Al}_y\text{O}_z:\text{Eu}^{2+}$ phosphor with various Al/Sr ratio.

<321 nm [24–26]. It related to crystal structure and luminescent mechanism and the reason will be explained below.

From Fig. 3, we could know the emission wavelength of these materials is controlled in 483–510 nm with increasing Al/Sr ratio and the luminescent color changes from green to blue. In order to prove again this result, the color coordinate pictures of the $\text{SrAl}_2\text{O}_4:\text{Eu}^{2+}$ (a) and $\text{Sr}_4\text{Al}_{14}\text{O}_{25}:\text{Eu}^{2+}$ (b) phosphors are shown in Fig. 4. The color coordinate of (x, y) is $(0.1261, 0.6282)$, $(0.1057, 0.2681)$ of $\text{SrAl}_2\text{O}_4:\text{Eu}^{2+}$ and $\text{Sr}_4\text{Al}_{14}\text{O}_{25}:\text{Eu}^{2+}$ phosphors, respectively [5, 27, 28]. The real photographs and the emission spectra of $\text{SrAl}_2\text{O}_4:\text{Eu}^{2+}$ and $\text{Sr}_4\text{Al}_{14}\text{O}_{25}:\text{Eu}^{2+}$ phosphors under excitation of UV light are shown in insets. From the insets, it is proved again that $\text{SrAl}_2\text{O}_4:\text{Eu}^{2+}$ phosphor and $\text{Sr}_4\text{Al}_{14}\text{O}_{25}:\text{Eu}^{2+}$ phosphor emit bright green and blue light, respectively.

The purity of color reflects the quality of phosphor. The higher its value is, the higher the quality is. Therefore, it is necessary to measure the purity of color of phosphor and improve its value as much as possible. The plotting method was taken to calculate the purity of color of $\text{SrAl}_2\text{O}_4:\text{Eu}^{2+}$ and $\text{Sr}_4\text{Al}_{14}\text{O}_{25}:\text{Eu}^{2+}$ phosphor, and the formulas are as follows:

$$P_a = \frac{\overline{aE}}{\overline{EP_1}} \quad (1)$$

$$P_b = \frac{\overline{bE}}{\overline{EP_2}} \quad (2)$$

Through the formulas and the coordinates of the white point $E(0.333, 0.333)$, the chrominance point of phosphor $a(0.1261, 0.6282)$ and $b(0.1057, 0.2681)$ and the dominant wavelength point $P_1(0.0236, 0.7732)$ and $P_2(0.0554, 0.2658)$, the highest color purity of $\text{SrAl}_2\text{O}_4:\text{Eu}^{2+}$ and $\text{Sr}_4\text{Al}_{14}\text{O}_{25}:\text{Eu}^{2+}$ phosphor is 0.6667 and 0.8229, respectively [29–31], which are pretty high and could satisfy the demand of production and living.

Effect of the concentration of Eu^{2+} ions on luminescent properties

Figure 5 shows the excitation (a) and emission (b) spectra of $\text{SrAl}_2\text{O}_4:x\text{Eu}^{2+}$ phosphors. The doping concentration of Eu^{2+} ions was 0.2, 0.5, 1.0, 2.0, 4.0, 6.0 at.%. The shapes of these excitation and emission spectra are basically identical for different Eu^{2+} ions concentration. The excitation range of these phosphors is from 280 to 440 nm, which has good absorption to UV and blue light, indicating these phosphors could be excited by UV and visible light. The excitation intensity firstly increases and then decreases with the increase in doping Eu^{2+} ions concentration, when the doping Eu^{2+} ions concentration approaches 0.5 at.%, the excitation intensity is the strongest and the excitation peak value wavelength is the shortest at 334 nm. However, while the doping concentration of Eu^{2+} ions is more than 0.5 at.%, the excitation peak begins redshift from 334

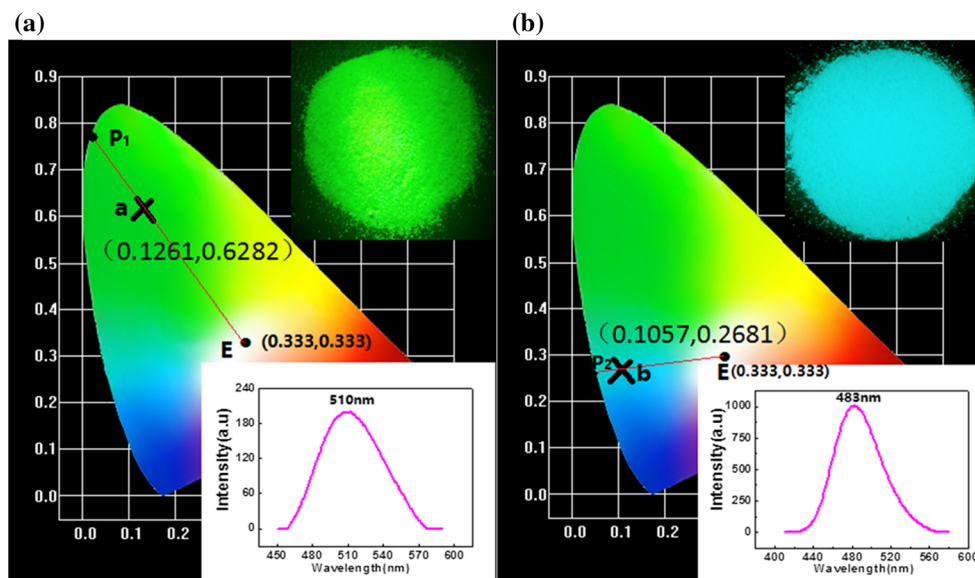


Figure 4 Color coordinate of samples when Al/Sr = 2 (a) and Al/Sr = 3.5 (b). *Insets* are the real photographs of phosphor and emission spectra under UV excitation.

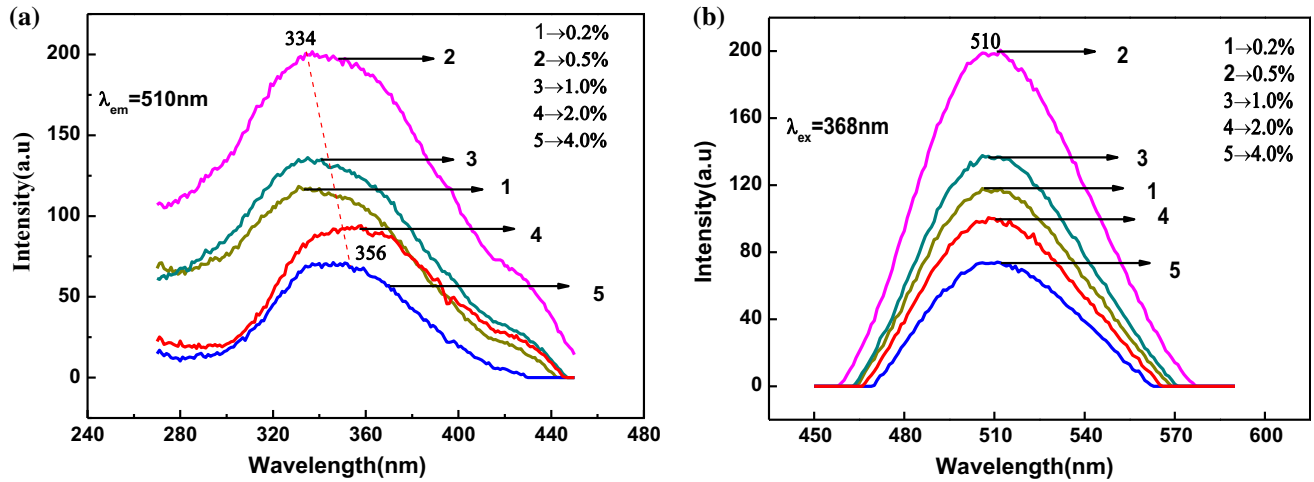


Figure 5 Excitation (a) and emission (b) spectra of SrAl₂O₄:Eu²⁺ phosphor with different Eu²⁺ ions doping.

to 356 nm. From the emission spectra, the emission peaks position of phosphors with different doping Eu²⁺ ions concentration are at about 510 nm. The doping of Eu²⁺ ions only effected on luminescent intensity. The emission intensity also firstly increases and then decreases with the increase in the Eu²⁺ ions concentration, and when the doping concentration of Eu²⁺ ions is 0.5 at.%, the emission intensity is the strongest. This is because a lot of Eu²⁺ ions enter crystal lattice at beginning, and they form more luminescent center, so the luminescent intensity is enhanced. When the doping concentration of Eu²⁺ ions is 0.5 at.%, the luminescent center reaches saturation and the luminescent intensity is significantly higher than the other proportion. Continuing increasing the concentration of Eu²⁺ ions, because

there are dislocation and crossed relaxation interaction, the energy will release as heat or other form, the luminescent intensity of the phosphors will be weakened [32–34]. Otherwise, because of the excessive luminescence center density, energy transfer rate is greater than the rate of fluorescent emission. The energy transfer appears between adjacent two Eu²⁺ ions through lattice vibration, which will be discussed on the quenching mechanism.

Figure 6 displays the excitation (a) and emission (b) spectra of Sr₄Al₁₄O₂₅:xEu²⁺ phosphors with the doping concentration of Eu²⁺ ions of 0.2, 0.5, 1.0, 2.0, 4.0, 6.0 at.%. The excitation spectra are composed of three areas, and there are two excitation peaks at 368 and 430 nm at area 2 and area 3, respectively. Combined with crystal structure, we thought that the

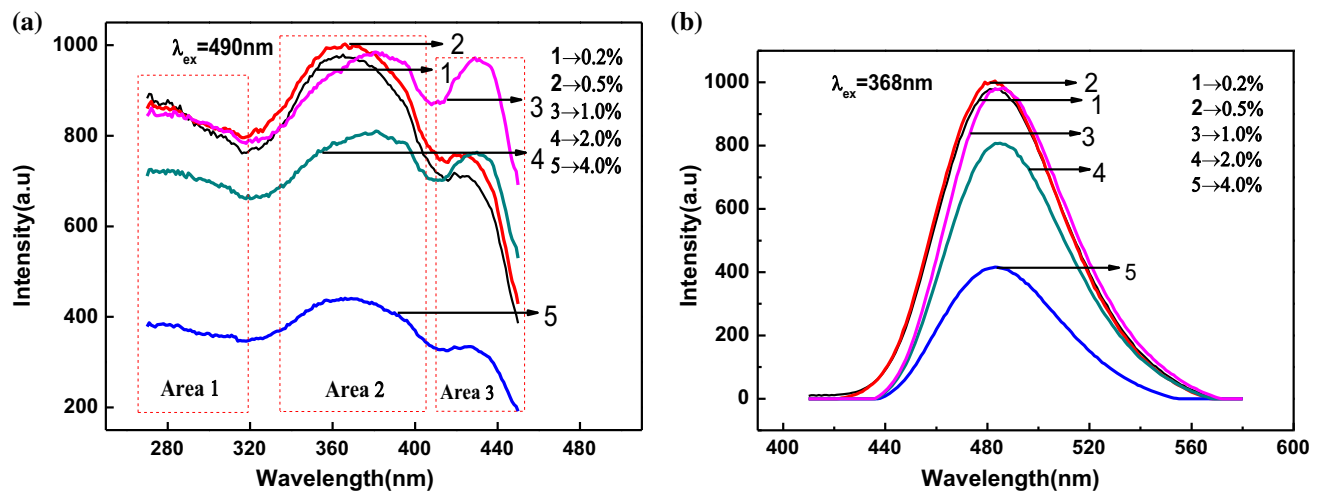


Figure 6 Excitation (a) and emission (b) spectra of Sr₄Al₁₄O₂₅:Eu²⁺ phosphor with different Eu²⁺ doping.

excitation at area 1 gives rise to the electric charge-transfer transition of phosphor matrix, since the band gap of $\text{Sr}_4\text{Al}_{14}\text{O}_{25}$ matrix is 6.3 eV [35, 36], which is larger than the excitation band, the excitation peaks at 368 and 430 nm are caused by the transition of ground state to excitation state of Eu^{2+} ions located at Sr1 and Sr2 lattice position, respectively. The excitation intensity firstly increases and then decreases with the increase in the doping concentration of Eu^{2+} ions. When the Eu^{2+} ions concentration is 0.2 at.%, the main excitation peaks are at 368 nm, but while the Eu^{2+} ions concentration is more than 0.2 at.%, the excitation peak at 430 nm is oppositely increased more than that of 368 nm. Especially, when the doping content of Eu^{2+} ions is 1.0 and 2.0 at.%, the excitation intensity of 430 nm is identical with that of 368 nm, indicating that these doping concentrations are benefit to the visible light excitation. There are no any changes in the shape of emission spectra, but the emission intensity increases firstly and then decreases with the increase in Eu^{2+} ions concentration. The spectral intensity is the lowest when the concentration of Eu^{2+} ions was 0.2 at.%. Continuing increasing concentration of Eu^{2+} ions, the spectral intensity increases somewhat. When the concentration of Eu^{2+} ions increases to 0.5 at.%, the emission intensity achieves largest. When the concentration of Eu^{2+} ions continues to increase, the emission intensity decreased gradually. The Eu^{2+} ions concentration is 0.5 at.% for the sample of the highest excitation and emission intensity.

When Eu^{2+} ions concentration is more than 0.5 at.%, the luminescent intensity begins to decrease.

Some analysis indicates there are some luminous centers in luminescent material, and the energy transfer will proceed in these luminescent center and crystal lattice. When the concentration of Eu^{2+} ions reaches certain value, the energy will transfer to in lattice. The following will discuss the relation between the energy transfer and fluorescent quenching. According to the theory of Dexter, the relation between luminescent intensity and the concentration of luminescent center of Eu^{2+} ions is shown in formula (3):

$$I/x = K \left[1 + \beta(\chi)^{Q/3} \right]^{-1} \quad (3)$$

In the formula, I represents light intensity, x represents luminescent center concentration; K and β are constant (under the condition of the same excitation). According to the interaction between the ions of luminescent center, Q value should be for 6, 8, 10 corresponding to the quenching mechanism of dipole–dipole interaction, dipole–quadrupole interaction, quadrupole–quadrupole interaction, respectively [37–39].

The formula (3) can be simplified to (4):

$$\lg(I/x) = c - (Q/3)\lg\chi \quad (4)$$

Based on the data of Figs. 5 and 6, the relation of $\lg(I/x)$ and $\lg(x)$ of $\text{SrAl}_2\text{O}_4:\text{Eu}^{2+}$ phosphors (a) and $\text{Sr}_4\text{Al}_{14}\text{O}_{25}:\text{Eu}^{2+}$ phosphors (b) is shown in Fig. 7 while x is more than 0.5. By means of liner fitting, the slope of curve is -1.4566 and -1.1998 of $\text{SrAl}_2\text{O}_4:\text{Eu}^{2+}$ and $\text{Sr}_4\text{Al}_{14}\text{O}_{25}:\text{Eu}^{2+}$ phosphor, respectively, so that the Q values of $\text{SrAl}_2\text{O}_4:\text{Eu}^{2+}$ and $\text{Sr}_4\text{Al}_{14}\text{O}_{25}:\text{Eu}^{2+}$ phosphor are 4.3698 and 3.5994, which is more

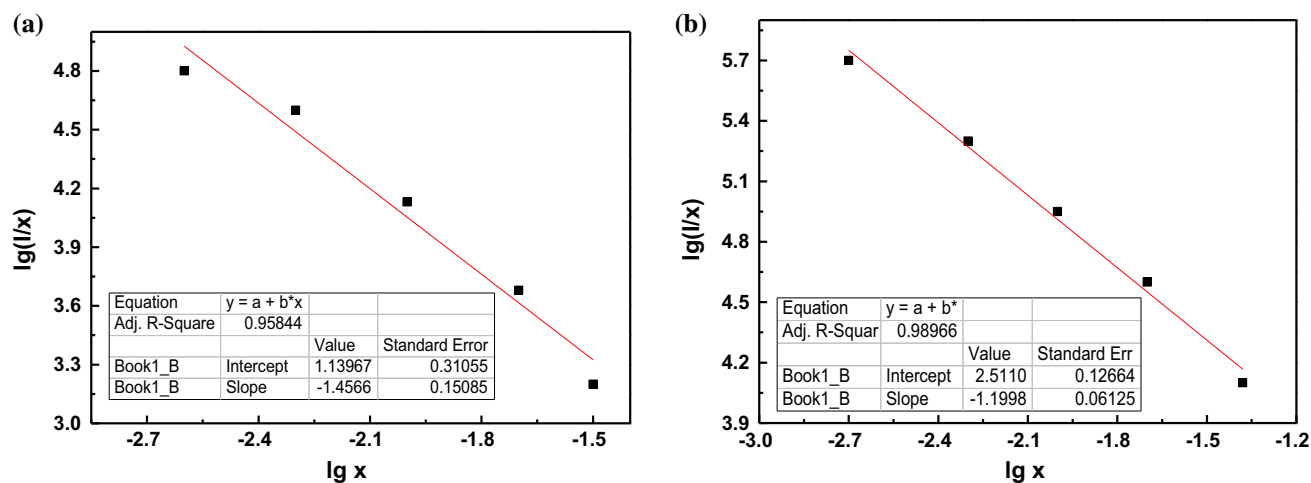


Figure 7 Relation between $\lg(x)$ and $\lg(I/x)$ of $\text{SrAl}_2\text{O}_4:\text{Eu}^{2+}$ (a) and $\text{Sr}_4\text{Al}_{14}\text{O}_{25}:\text{Eu}^{2+}$ (b) phosphors.

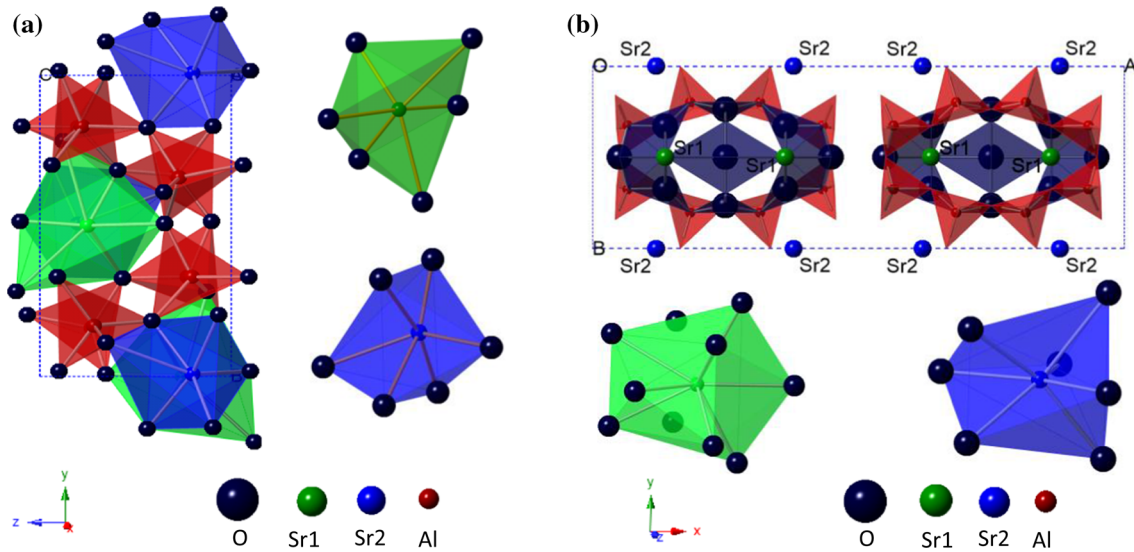


Figure 8 Unit cell and local coordination geometry environment of Sr²⁺ of SrAl₂O₄ (a) and Sr₄Al₁₄O₂₅ (b).

near to 6. Therefore, the concentration quenching mechanism of Eu²⁺ ions in SrAl₂O₄:Eu²⁺ and Sr₄Al₁₄O₂₅:Eu²⁺ phosphors can only belong to the dipole–dipole interaction.

The luminescence mechanism of SrAl₂O₄:Eu²⁺ and Sr₄Al₁₄O₂₅:Eu²⁺ phosphors

In order to better explain the spectral properties of SrAl₂O₄:Eu²⁺ and Sr₄Al₁₄O₂₅:Eu²⁺ phosphors, the crystal structure and coordination geometry of SrAl₂O₄ and Sr₄Al₁₄O₂₅ are constructed and are shown in Fig. 8. Figure 8a is the unit cell and local coordination geometry environment of Sr²⁺ in SrAl₂O₄ crystal, and Fig. 8b is that in Sr₄Al₁₄O₂₅ crystal. SrAl₂O₄ belongs to monoclinic system with a space group of P2₁, the lattice parameters are $a = 0.8442$ nm, $b = 0.8822$ nm and $c = 0.5161$ nm, and the angle of cell is 93.415°. In unit cell of SrAl₂O₄, the structure consists of AlO₄ tetrahedra and strontium ions are filled in the interstice formed by the AlO₄ tetrahedra. Every unit cell contains two species strontium ionic coordination polyhedron with the same coordination number and similar average Sr–O distances. Every Sr²⁺ ion forms asymmetric octahedron with surrounding six adjacent oxygen ions. Despite all that, there are two lattice position of Sr²⁺ ion in an unit cell, but only one luminescent property when Eu²⁺ ions substitute different Sr²⁺ ions. Sr₄Al₁₄O₂₅ is orthorhombic crystal structure with a

Pmma space group, and the lattice parameters are $a = 2.4785$ nm, $b = 0.8487$ nm and $c = 0.4886$ nm. In unit cell of Sr₄Al₁₄O₂₅, the structure consists of AlO₆ octahedra which separated by a double layer of AlO₄ tetrahedra. There are two species of strontium ionic coordination polyhedron with coordination numbers 10 and 7 in every unit cell. Therefore, when Eu²⁺ ions replace Sr²⁺ ions, there are two different types of luminescent Eu²⁺ centers. The average Sr–O bond length of tenfold coordinated strontium marked Sr1 (2.77 Å) is longer than that of the sevenfold coordinated strontium marked Sr2 (2.62 Å), and the interactions between oxygen and strontium ions at the tenfold coordinated site will be weaker than for the sevenfold coordinated site. Because of the different local environments (based on the coordination number) of Eu²⁺ ions substituting different Sr²⁺ ions, there are two Eu²⁺ luminescence centers named Eu1 and Eu2 which occupy Sr1 and Sr2 lattice position, respectively. Due to the shorter Sr–O distances, there are the higher covalency and the larger crystal field splitting for Eu2 in the sevenfold coordinated site than for Eu1 in the tenfold coordinated site, and the band gap of Eu²⁺ from ground state to excitation state is narrow [40–42]. In order to confirm the result, the emission spectra of Sr₄Al₁₄O₂₅:Eu²⁺ phosphor doped with 0.5 and 1.0 at.% Eu²⁺ ion were analyzed again through Guess fitting. The results are shown in supplement Figs. S5 and S6. It is concluded that there are two excitation peaks except the excitation band excitation wavelength which is shorter than 320 nm.

While doping 0.5 at.% Eu^{2+} ion, the excitation peak is at 360 and 431 nm; however, while doping 1.0 at.% Eu^{2+} ion, the excitation peak is at 376 and 432 nm, respectively. In addition, the long wavelength of 432 nm excitation apparently enhances and the short wavelength excitation extends from 360 to 376 nm, which indicates that more Eu^{2+} ion occupies Sr2 lattice site; simultaneously, the Sr2 lattice site is stretched since the ionic radius of Eu^{2+} (0.947 Å) is less than that of Sr^{2+} (1.12 Å).

Figure 9 shows the excitation and emission spectra and wave numbers of $\text{SrAl}_2\text{O}_4:\text{Eu}^{2+}$ (a) and $\text{Sr}_4\text{Al}_{14}\text{O}_{25}:\text{Eu}^{2+}$ (b) phosphor. The Stokes frequency shift between the excitation and emission spectra of $\text{SrAl}_2\text{O}_4:\text{Eu}^{2+}$ is 10333 cm^{-1} (176 nm). However, in the $\text{Sr}_4\text{Al}_{14}\text{O}_{25}:\text{Eu}^{2+}$ phosphor, the shortest Stokes frequency shift is 2553 cm^{-1} (53 nm) and the longest is only 6470 cm^{-1} (115 nm) corresponding to Eu2 and Eu1, respectively, which indicates that the frequency shift decreases with the increase in Al/Sr ratio and the non-radiation transition descends originated from the compressing of $5d$ energy level splitting. In order to best explain the changeable rule of phosphor spectrum, combining established crystal structure of $\text{SrAl}_2\text{O}_4:\text{Eu}^{2+}$ and $\text{Sr}_4\text{Al}_{14}\text{O}_{25}:\text{Eu}^{2+}$ phosphor, the energy band and transition of Eu^{2+} ion is built and shown in Fig. 10. The electron configuration of Eu^{2+} ion is Xe atomic configuration plus $4f^75s^25p^6$. There are seven f shell electrons in the ground state of Eu^{2+} ion, and the $4f^7$ electrons organize themselves into $4f^7$ configurations, and the ground-state level is decided by Hund rule. First of all, the electron spin in the

lowest energy state should be parallel as much as possible, that is, the total spin angular momentum quantum number S should be the biggest. Secondly, on the premise of S for the biggest, the total orbital angular momentum L should be minimum. There are seven electrons in one Eu^{2+} ion, and all the electron spin is parallel, so $S = 7/2$, $L = 0$. Therefore, we get its ground-state spectral term of $^8S_{7/2}$, defining the spectral term overlaps with valence top of SrAl_2O_4 and $\text{Sr}_4\text{Al}_{14}\text{O}_{25}$ crystal. The band gap of SrAl_2O_4 and $\text{Sr}_4\text{Al}_{14}\text{O}_{25}$ crystal is 6.6 and 6.3 eV, which is far higher than the excitation state of Eu^{2+} ion; therefore, the band gap transition is in existence. For Eu^{2+} ion, the $4f^65d^1$ electronic configuration forms when it is excited due to the shielding effect of $5s^25p^6$ electrons. Affected by crystal field, the low energy level of $4f^65d^1$ generates splitting, and the energy level splitting becomes large with the decrease in coordination number and symmetry. When coordination number is 6, the energy level splitting arrives to 1.29 eV, when the coordination number is 7, the energy level splitting is 0.78 eV; however, when the coordination number is 10, the energy level splitting is only 0.31 eV. Therefore, the relation of energy level splitting and coordination number can be expressed as E_6 (6-coordination) $>$ E_7 (7-coordination) $>$ E_{10} (10-coordination) in aluminate phosphor. For this reason, the different crystal field environment of Eu^{2+} ion brings the different forms of electron transition [43, 44]. In the $\text{Sr}_4\text{Al}_{14}\text{O}_{25}:\text{Eu}^{2+}$ phosphor, only one emission peak for the two Eu^{2+} ion lattice positions indicates there is the same energy band bottom of

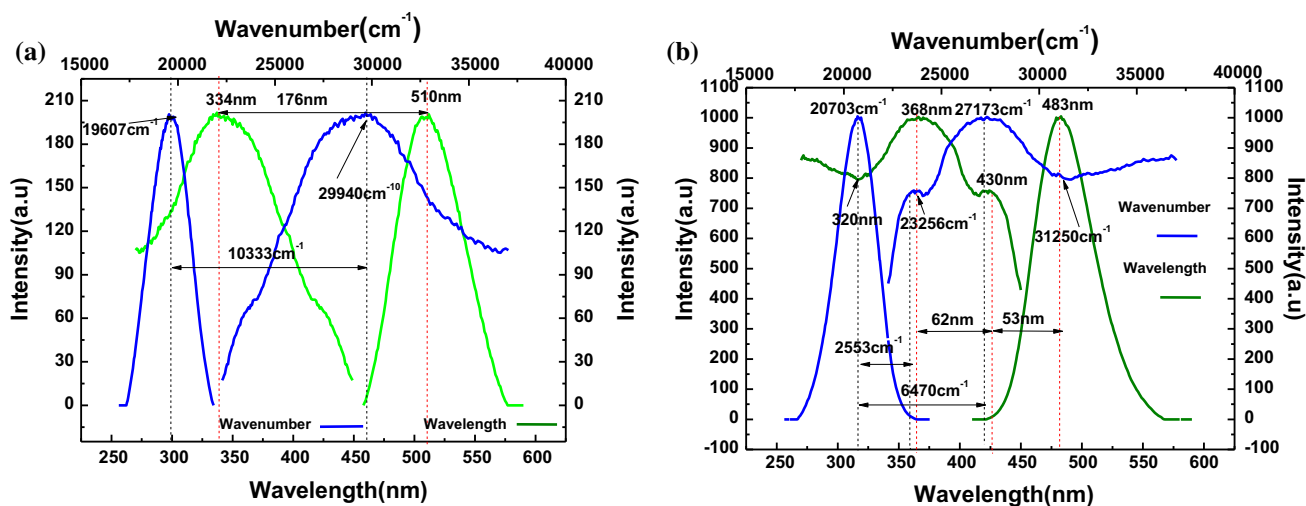


Figure 9 Excitation and emission spectra and wave numbers of $\text{SrAl}_2\text{O}_4:\text{Eu}^{2+}$ (a) and $\text{Sr}_4\text{Al}_{14}\text{O}_{25}:\text{Eu}^{2+}$ (b) phosphor.

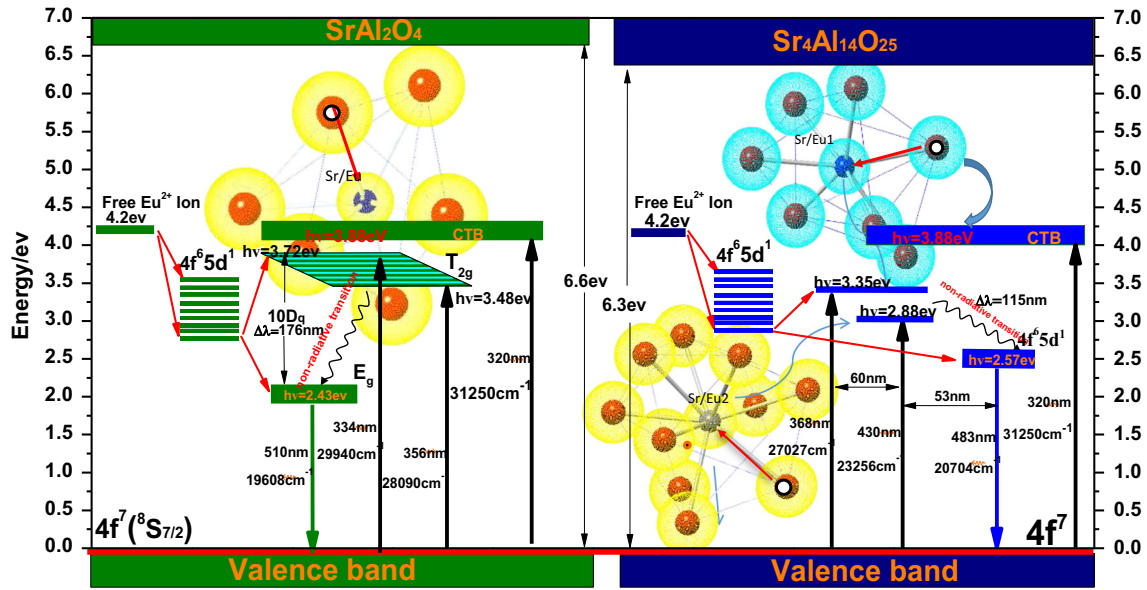


Figure 10 Energy level models of $\text{SrAl}_2\text{O}_4:\text{Eu}^{2+}$ and $\text{Sr}_4\text{Al}_{14}\text{O}_{25}:\text{Eu}^{2+}$ phosphor.

Eu1 and Eu2 luminescent centers. However, there are two excitation peaks caused by the transition from identical ground state to the excitation tops of Eu1 and Eu2 coming from the crystal field splitting, indicating coordination field only affects the energy top of crystal field splitting. Larger coordination number is, lower the energy level top of crystal field splitting in $\text{Sr}_4\text{Al}_{14}\text{O}_{25}:\text{Eu}^{2+}$ phosphor is. When excitation wavelength is <320 nm, the Al–O group transfers one electron to centric cation forming the charge-transfer-band transition, and the lowest charge-transfer energy is 3.88 eV.

Conclusions

Phosphors based on strontium aluminates activated by Eu^{2+} ions with various Al/Sr ratios were synthesized by the high-temperature solid-state method. The optimum synthetic temperature and time are about 1350 °C and 3.5 h. At the range of Al/Sr ratio from 1.5 to 4.0, there are only three crystal structures, cubic (1.5), monoclinic (2.0–3.0) and orthorhombic (3.0–4.0) phases. Under UV light excitation, the emission peaks gradually generate blueshift from 510 nm of $\text{Sr}_3\text{Al}_2\text{O}_6:\text{Eu}^{2+}$ phosphor to 483 nm of $\text{Sr}_4\text{Al}_{14}\text{O}_{25}:\text{Eu}^{2+}$ phosphor and the two emission peaks are originated from $4f^6 5d^1$ to $4f^7$ intrinsic transition of Eu^{2+} ions. The best green and blue luminescent samples are $\text{SrAl}_2\text{O}_4:\text{Eu}^{2+}$ and $\text{Sr}_4\text{Al}_{14}\text{O}_{25}:\text{Eu}^{2+}$, and

their color purity is 0.6667 and 0.8229, respectively. The best doping amount of Eu^{2+} is 0.5 at.%, and the concentration quenching mechanism of Eu^{2+} ions in $\text{SrAl}_2\text{O}_4:\text{Eu}^{2+}$ and $\text{Sr}_4\text{Al}_{14}\text{O}_{25}:\text{Eu}^{2+}$ phosphors can be ascribed to the dipole–dipole interaction. There are three types of 6, 7 and 10 coordination numbers around Sr^{2+} (Eu^{2+}) ion, which forms three types of polyhedras, resulting in generating three excitation peaks at 334, 368 and 430 nm corresponding to the 6, 7 and 10 coordination polyhedral. The relation of energy level splitting and coordination number can be expresses as E_6 (6-coordination) $> E_7$ (7-coordination) $> E_{10}$ (10-coordination) in aluminate phosphor, and the splitting width of 6, 7 and 10 coordination numbers is 1.29, 0.78 and 0.31 eV, respectively. The coordination field only affects the energy top of crystal field splitting, and the larger the coordination number is, the lower the energy level top of crystal field splitting in $\text{Sr}_4\text{Al}_{14}\text{O}_{25}:\text{Eu}^{2+}$ phosphor is. These results can be a fundament of wavelength tuning of strontium aluminate phosphor.

Acknowledgements

This work was supported by the Projects of the National Natural Science foundation of China (Nos. 51602027, 61307118), of Jilin Science and Technology Bureau (No. 201201117), of Changchun Science and Technology Bureau (No. 2013045).

Electronic supplementary material: The online version of this article (doi:10.1007/s10853-017-1027-4) contains supplementary material, which is available to authorized users.

References

- [1] Zhang X, Wang J, Huang L, Pan F, Chen Y, Lei B, Wu M (2015) Tunable luminescent properties and concentration-dependent, site-preferable distribution of Eu^{2+} ions in silicate glass for white LEDs applications. *ACS Appl Mater Interfaces* 7:10044–10054
- [2] Palilla FC, Levine AK, Tomkus MR (1968) Fluorescent properties of alkaline earth aluminates of the type MAI_2O_4 activated by divalent europium. *J Electrochem Soc* 115:642–644
- [3] Matsuzawa T, Aoki Y, Takeuchi N, Murayama Y (1996) A new long phosphorescent phosphor with high brightness, $\text{SrAl}_2\text{O}_4:\text{Eu}^{2+}, \text{Dy}^{3+}$. *J Electrochem Soc* 143:2670–2673
- [4] Feng X, Feng W, Wang K (2015) Experimental and theoretical spectroscopic study of praseodymium(III) doped strontium aluminate phosphors. *J Alloys Compd* 628:343–346
- [5] Van den Eeckhout K, Smet PF, Poelman D (2010) Persistent luminescence in Eu^{2+} -doped compounds: a review. *Materials* 3:2536–2566
- [6] Li YQ, Hintzen HT (2006) Luminescence properties of Eu^{2+} -doped $\text{MAI}_{2-x}\text{Si}_x\text{O}_{4-x}\text{N}_x$ ($M = \text{Ca}, \text{Sr}, \text{Ba}$) conversion phosphor for white LED applications. *J Electrochem Soc* 153:278–282
- [7] Lin Y, Tang Z, Zhang Z (2001) Preparation of long-afterglow $\text{Sr}_4\text{Al}_{14}\text{O}_{25}$ -based luminescent material and its optical properties. *Mater Lett* 51:14–18
- [8] Alahraché S, Al Saghir K, Chenu S, Veron E, de Sousa Meneses D, Becerro AI, Cusso F (2013) Perfectly transparent $\text{Sr}_3\text{Al}_2\text{O}_6$ polycrystalline ceramic elaborated from glass crystallization. *Chem Mater* 25:4017–4024
- [9] Gao HM, Yan FY, He L (2015) Synthesis and luminescence property of $\text{Sr}_3\text{Al}_2\text{O}_6:\text{Eu}^{3+}$ red phosphor prepared by coprecipitation technique. *Adv Mater Res* 1096:486–491
- [10] Page P, Ghildiyal R, Murthy KVR (2006) Synthesis, characterization and luminescence of $\text{Sr}_3\text{Al}_2\text{O}_6$ phosphor with trivalent rare earth dopant. *Mater Res Bull* 41:1854–1860
- [11] Zhang P, Li L, Xu M, Liu L (2008) The new red luminescent $\text{Sr}_3\text{Al}_2\text{O}_6:\text{Eu}^{2+}$ phosphor powders synthesized via sol-gel route by microwave-assisted. *J Alloys Compd* 456:216–219
- [12] Zhong R, Zhang J, Zhang X, Lu S, X-j Wang (2006) Red phosphorescence in $\text{Sr}_4\text{Al}_{14}\text{O}_{25}$: $\text{Cr}^{3+}, \text{Eu}^{2+}, \text{Dy}^{3+}$ through persistent energy transfer. *Appl Phys Lett* 88:201916
- [13] Dutczak D, Ronda C, Justel T, Meijerink A (2014) Anomalous trapped exciton and $d-f$ emission in $\text{Sr}_4\text{Al}_{14}\text{O}_{25}:\text{Eu}^{2+}$. *J Phys Chem A* 118:1617–1621
- [14] Garcia CR, Oliva J, Romero MT, Diaz-Torres LA (2016) Enhancing the photocatalytic activity of $\text{Sr}_4\text{Al}_{14}\text{O}_{25}:\text{Eu}^{2+}, \text{Dy}^{3+}$ persistent phosphors by codoping with Bi^{3+} ions. *Photochem Photobiol* 92:231–237
- [15] Chang C, Li W, Huang X, Wang Z, Chen X, Qian X, Mao D (2010) Photoluminescence and afterglow behavior of $\text{Eu}^{2+}, \text{Dy}^{3+}$ and $\text{Eu}^{3+}, \text{Dy}^{3+}$ in $\text{Sr}_3\text{Al}_2\text{O}_6$ matrix. *J Lumin* 130:347–350
- [16] Inan Akmeahmet G, Šturm S, Bocher L, Kociak M, Ambrožič B, Ow-Yang CW (2016) Structure and luminescence in long persistence Eu, Dy, and B codoped strontium aluminate phosphors: the boron effect. *J Am Ceram Soc* 99:2175–2180
- [17] Zhang J, Ge M (2011) Effecting factors of the emission spectral characteristics of rare-earth strontium aluminate for anti-counterfeiting application. *J Lumin* 131:1765–1769
- [18] Kshatri DS, Khare A (2014) Characterization and optical properties of Dy^{3+} doped nanocrystalline $\text{SrAl}_2\text{O}_4:\text{Eu}^{2+}$ phosphor. *J Alloys Compd* 588:488–495
- [19] Sahu IP, Bisen DP, Brahme N, Tamrakar RK (2016) Luminescence behavior of europium activated strontium aluminate phosphors by solid state reaction method. *J Mater Sci Mater Electron* 27:3443–3455
- [20] Mishra SB, Mishra AK, Revaprasadu N, Hillie KT, Steyn WV, Coetsee E, Swart HC (2009) Strontium aluminate/polymer composites: morphology, luminescent properties, and durability. *J Appl Polym Sci* 112:3347–3354
- [21] Dutczak D, Jüstel T, Ronda C, Meijerink A (2015) Eu^{2+} luminescence in strontium aluminates. *Phys Chem Chem Phys* 17:15236–15249
- [22] Ma W, Wan FR, Long Y, Shang CJ (2003) Relation between luminescence and granularity of $\text{SrAl}_2\text{O}_4:\text{Eu}, \text{Dy}$. *Faguang Xuebao Chin J Lumin* 24:95–99
- [23] Akiyama M, Xu CN, Liu Y, Nonaka K, Watanabe T (2002) Influence of Eu, Dy co-doped strontium aluminate composition on mechanoluminescence intensity. *J Lumin* 97:13–18
- [24] Aitasalo T, Dereń P, Hölsä J, Jungner H, Krupa JC, Lastusaari M, Stręk W (2003) Persistent luminescence phenomena in materials doped with rare earth ions. *J Solid State Chem* 171:114–122
- [25] Luo X, Cao W, Xiao Z (2006) Investigation on the distribution of rare earth ions in strontium aluminate phosphors. *J Alloys Compd* 416:250–255
- [26] Xingdong LÜ, Wangen SHU (2007) Roles of crystal defects in the persistent luminescence of $\text{Eu}^{2+}, \text{Dy}^{3+}$ co-doped strontium aluminate based phosphors. *Rare Met* 26:305–310
- [27] Clabau F, Rocquefelte X, Jobic S, Deniard P, Whangbo MH, Garcia A, Le Mercier T (2005) Mechanism of

- phosphorescence appropriate for the long-lasting phosphors Eu^{2+} -doped SrAl_2O_4 with codopants Dy^{3+} and B^{3+} . *Chem Mater* 17:3904–3912
- [28] Shaheen SE, Jabbour GE, Morrell MM, Kawabe Y, Kippelen B, Peyghambarian N, Armstrong NR (1998) Bright blue organic light-emitting diode with improved color purity using a LiF/Al cathode. *J Appl Phys* 84:2324–2327
- [29] Wondraczek L, Krolkowski S, Nass P (2013) Europium partitioning, luminescence re-absorption and quantum efficiency in (Sr, Ca) åkermanite—feldspar bi-phasic glass ceramics. *J Mater Chem C* 1:4078–4086
- [30] Ho CL, Wong WY, Gao ZQ, Chen CH, Cheah KW, Yao B, Yu XM (2008) Red-light-emitting iridium complexes with hole-transporting 9-arylcarbazole moieties for electrophosphorescence efficiency/color purity trade-off optimization. *Adv Func Mater* 18:319–331
- [31] Feng J, Li F, Gao Cheng G, Xie W, Liu S (2002) Improvement of efficiency and color purity utilizing two-step energy transfer for red organic light-emitting devices. *Appl Phys Lett* 81:2935–2937
- [32] Sugar J, Spector N (1974) Spectrum and energy levels of doubly ionized europium (Eu III). *JOSA* 64:1484–1497
- [33] Hölsä J, Laamanen T, Lastusaari M, Niittykoski J, Novák P (2009) Electronic structure of the $\text{SrAl}_2\text{O}_4:\text{Eu}^{2+}$ persistent luminescence material. *J Rare Earths* 27:550–554
- [34] Chandra BP, Sonwane VD, Haldar BK, Pandey S (2011) Mechanoluminescence glow curves of rare-earth doped strontium aluminate phosphors. *Opt Mater* 33:444–451
- [35] Luan L, Guo CF, Huang DX (2009) Effect of Al/Sr ratio on properties of strontium aluminate long lasting phosphor. *J Inorg Mater* 24:53–56
- [36] Minquan W, Wang D, Guangle L (1998) Research on fluorescence spectra and structure of single-phase $4\text{SrO}\cdot 7\text{Al}_2\text{O}_3:\text{Eu}^{2+}$ phosphor prepared by solid-state reaction method. *Mater Sci Eng B* 57:18–23
- [37] Li X, Budai JD, Liu F, Chen YS, Howe JY, Sun C, Pan Z (2015) Crystal structures and optical properties of new quaternary strontium europium aluminate luminescent nanoribbons. *J Mater Chem C* 3:778–788
- [38] Komatsu K, Nakamura A, Kato A, Ohshio S, Saitoh H (2015) Blue phosphor synthesized with Eu-containing strontium aluminate by reaction on single crystalline magnesia. *Phys Status Solidi (c)* 12:809–813
- [39] Kaya SY, Karacaoglu E, Karasu B (2012) Effect of Al/Sr ratio on the luminescence properties of $\text{SrAl}_2\text{O}_4:\text{Eu}^{2+}$, Dy^{3+} phosphors. *Ceram Int* 38:3701–3706
- [40] Wu S, Zhang S, Liu Y, Yang J (2007) The organic ligands coordinated long afterglow phosphor. *Mater Lett* 61:3185–3188
- [41] Kshatri DS, Khare A (2014) Optical properties of rare earth doped strontium aluminate (SAO) phosphors: a review. *Opt Spectrosc* 117:769–783
- [42] Sharma SK, Pitale SS, Malik MM, Dubey RN, Qureshi MS (2008) Synthesis and detailed kinetic analysis of $\text{Sr}_4\text{Al}_{14}\text{O}_{25}:\text{Eu}^{2+}$ phosphor under black light irradiation. *Radiat Eff Defects Solids* 163:767–777
- [43] Yoon S, Bierwagen J, Trottmann M, Walfort B, Gartmann N, Weidenkaff A, Pokrant S (2015) The influence of boric acid on improved persistent luminescence and thermal oxidation resistance of $\text{SrAl}_2\text{O}_4:\text{Eu}^{2+}$. *J Lumin* 167:126–131
- [44] Rojas-Hernandez RE, Rodriguez MA, Rubio-Marcos F, Serrano A, Fernandez JF (2015) Designing nanostructured strontium aluminate particles with high luminescence properties. *J Mater Chem C* 3:1268–1276